Fast Backward Drift of Pellet Ablatant in Tokamak Plasmas

J. de Kloe, E. Noordermeer, N. J. Lopes Cardozo, and A. A. M. Oomens
FOM-Instituut voor Plasmafysica "Rijnhuizen," Association Euratom-FOM, Trilateral Euregio Cluster, P.O. Box 1207, 3430 BE Nieuwegein, The Netherlands
(Received 30 November 1998)

Pellet ablation in the Rijnhuizen Tokamak Project has been studied with an array of 16 fibers viewing the pellet trajectory along very narrow lines of sight. Rapid backward drift of the ablation cloud away from the pellet was observed. This has implications for the determination of the fueling profile and the penetration of the pellet in the plasma. Furthermore, this movement of the ablation cloud offers a new explanation for the often observed striations in the light emission. In contrast to the picture of the pellet periodically leaving the ablation cloud, the ablation cloud moves periodically away from the pellet. [S0031-9007(99)08796-7]

PACS numbers: 52.55.Fa, 28.52.Cx, 52.30.–q, 52.70.–m

One of the outstanding problems in thermonuclear fusion research is the fueling of the burning plasma. The high speed (several km/s) injection of pellets of solid hydrogen isotopes is one of the options. To obtain reliable models to predict the local fueling rate, the present pellet ablation theories must be validated. Much experimental and theoretical work still has to be done since large discrepancies have been reported between the ablation rate as measured by different diagnostics. For example, fueling measured by Thomson scattering at the Joint European Torus showed a fueling located primarily at the edge of the plasma, while the line emission (Balmer alpha line), which is usually taken as a measure for the ablation rate, placed the fueling in the inner parts of the plasma [1].

In the Rijnhuizen Tokamak Project (RTP) [2], the ablation of the pellet was monitored by two diagnostics. The intensity of the H_α emission from the ablation cloud was measured as a function of time by a detector viewing a large plasma volume, and as a function of position by taking time integrating photographs. Between these two measurements sometimes a discrepancy in the observed pellet penetration was found.

A dedicated diagnostic has been built to clarify this discrepancy. It consists of a row of 16 fibers viewing the pellet trajectory along narrow lines of sight, resulting in a very high spatial and temporal resolution. This is necessary because the shape of the cloud is observed to change within intervals of a few μs [3]. Properties that can be measured with this diagnostic are pellet velocity, ablation cloud size and position, and penetration depth.

Experimental setup.—The experiments were carried out in the RTP tokamak (major radius $R = 0.72$ m, minor radius $a = 0.164$ m, toroidal magnetic field $B_{\mathrm{tor}} \leq 2.4$ T, plasma current $I_{\mathrm{pl}} \leq 150$ kA, effective ion charge $Z_{\mathrm{eff}} \approx 1.5$–$3.0$, circular cross section). Typical plasma parameters are central electron temperature and density $T_{e,0} \approx 0.7$ keV, $n_{e,0} \approx 5 \times 10^{19}$ m^{-3} for plasmas with Ohmic heating (measured with Thomson scattering [4] and interferometry [5]). With central electron cyclotron heating (ECH) (≤ 350 kW, 2nd harmonic heating at 110 GHz) $T_{e,0} = 1.5$–2 keV is reached at $n_{e,0} = 5 \times 10^{19}$ m^{-3}. With off-axis ECH very broad, flat, or slightly hollow T_e profiles are obtained with $T_e \leq 0.5$ keV everywhere [6]. Thus, target plasmas with a large T_e range can be made, allowing the study of ablation in different conditions.

Pellets of 0.5 and 2.0×10^{19} atoms in size (m_{pellet}), with velocities (v_{pellet}) between 500 and 1000 m/s, and radius (r_{pellet}) of 0.3 or 0.4 mm have been used. The existing diagnostics are the photographic camera (resolution 1 mm, no time resolution) and the wide angle fibers (time resolution 0.5 μs, no spatial resolution) viewing the H_α line emission, as shown in Fig. 1. For the new diagnostic a row of 16 fibers was mounted in one of the image planes of the lens system, on the line where the pellet trajectory is imaged (see Fig. 1).

To narrow the lines of sight of the fibers a black block of 40 mm thickness, with 1 mm diameter holes in it, was

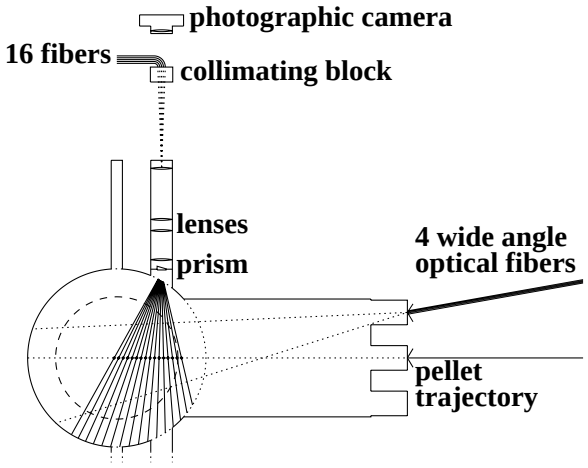

FIG. 1. Overview of the experimental setup in a poloidal cross section of the tokamak. Shown are the photographic camera, the wide angle fibers, and the new diagnostic, consisting of the 16 fibers and a collimating block to narrow the lines of sight. The viewing lines of the new fiber array diagnostic are indicated by the fan of lines originating from the prism. The dashed circle indicates the plasma boundary. The pellet moves inward along the major radius of the torus.

mounted in front of the fibers. This resulted in narrow lines of sight for the fibers, about 3.5 mm on the actual pellet trajectory for horizontal injection. The separation of the fibers was 4.5 mm in the image plane which resulted in a spatial separation of the viewing lines of 9.6 mm on the actual pellet trajectory for horizontal pellet injection.

The toroidal dimension of the viewing spots is also 3.5 mm, the centers of the spots are aligned to within 10 mm of the pellet trajectory. Given the extension of the ablation cloud in toroidal direction, this could lead to a systematic variation of the measured intensity along the array of up to 50%, varying smoothly from channel to channel. Such an error on the amplitude of the signals has no bearing on the analysis and conclusions presented in this Letter. Measurements with the photographic camera showed that the deviation of the pellet trajectory in toroidal direction is negligible in the conditions at hand.

The signals from all 16 fibers are measured independently using photodiodes. The temporal resolution of the system was 1 μs, determined by the analog-to-digital converters.

A relative calibration of the channels was determined by taking measurements of a pellet shot with quiet ablation, showing only one peak on most channels (see Fig. 2) and assuming the peak height to be equal to the large angle H_α signal at the same time.

Results in different plasma regimes.—Following the commonly accepted picture of a cigar shaped ablation cloud which is localized in major radial direction around the actual pellet position, we expect each of the channels to give a short pulse. The width of the pulse should then be a measure of the ablation cloud dimensions in major radial direction. This is indeed seen for pellets injected in low temperature plasmas ($T_e \leq 400$ eV). This situation can be obtained by injecting the pellet off-axis or by injecting in a plasma shortly after a period of off-axis ECH [6]. An example of the second type is shown in Fig. 2. As the pellet passes the viewing lines of the different channels clearly a pulse of light is observed, showing that the ablation cloud is located close to the pellet in major radial direction. The onset of these pulses coincides with the pellet velocity and timing as determined inside the pellet injector. The average width of the pulses on each channel is 16 ± 5 μs corresponding to a width of the ablation cloud of $\approx$12 mm. The velocity measured with the new diagnostic is 980 ± 25 m/s, in agreement with the value measured inside the injector (962 ± 1 m/s). The uncertainty is mostly systematic and due to the position calibration of the viewing lines. From the last visible pulse (on channel 2) it follows that the penetration of the pellet was $\approx 15.0 \pm 0.5$ cm. This agrees with the value obtained by the end of the wide angle H_α signal yielding a value of 15 ± 1 cm.

The result shown in Fig. 2 excludes the possibility of reflections playing a role. This has been confirmed by ray tracing calculations.

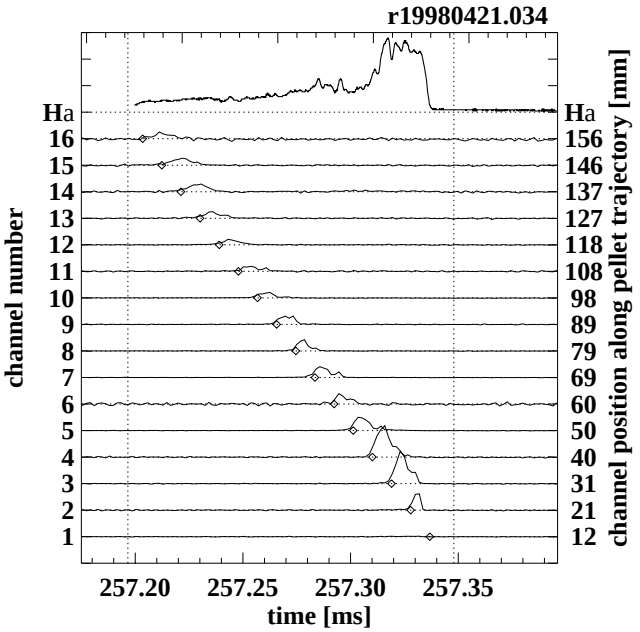

FIG. 2. Example of the pellet ablation process as observed by the fiber array for a pellet injected in a relatively cold plasma (7 ms after switch off of off-axis ECH [6]). The diamonds indicate the expected passage times of the pellet using the measured pellet velocity and timing in the injector. The vertical dashed lines indicate the moments that the pellet passes the limiter radius and the plasma center (if it would penetrate that far). The top trace is the wide angle H_α monitor. A clear peak is seen at the passage of the pellet at each channel. The pellet and plasma parameters are $n_{e,0} = 5.7 \times 10^{19}$ m^{-3}, $T_{e,0} =$ 280 eV, $I_{\rm pl} = 84.3$ kA, $B_{\rm tor} = 2.27$ T, $Z_{\rm eff} = 1.7$, $v_{\rm pellet} =$ 962 m/s, $m_{\rm pellet} = 0.5 \times 10^{19}$ atoms, $r_{\rm pellet} = 0.3$ mm.

A second example is given for normal Ohmic plasma conditions. This gives a completely different picture (see Fig. 3). Here the pulses are much broader in all channels. Besides that, separate peaks can be distinguished after the passage of the pellet, which we will refer to as secondary peaks. These are clearly correlated in different channels (see, for example, the parallelogram in Fig. 3). Assuming these secondary peaks are caused by an object moving through the plasma along the pellet trajectory a velocity can be calculated. For the highlighted peaks the velocity was 3.5 km/s. In other cases it has been observed to be as high as 10 km/s. With this velocity and the known resolution of the system the size of the object can be calculated to be $\approx$14 mm (channel 12). The size decreases as it moves outward on the subsequent channels. In this case the pellet penetrates beyond the reach of the diagnostic so no penetration depth can be determined here.

A third example shows the results for a pellet injected in a plasma during central ECH (320 kW) (see Fig. 4). Here the secondary peaks are much stronger than in the Ohmic case (the sensitivity along the y scale is reduced by 50% compared to Figs. 2 and 3). The secondary peaks persist longer than the primary ones. The pellet penetration found

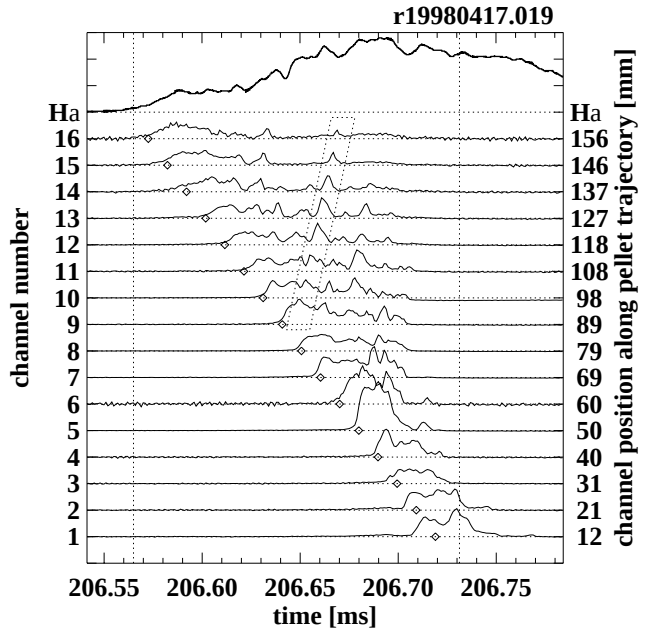

FIG. 3. Example of the pellet ablation process as observed by the new fiber-array diagnostic for an Ohmic plasma, plotted in the same way as in Fig. 2. Besides much broader peaks at all channels after passage of the pellet also a substructure of peaks can be recognized which are correlated on separate channels. An example of this is highlighted by the overplotted parallelogram. This sequence of correlated peaks shows the presence of a light source which moves faster than the pellet and in the opposite direction. The pellet and plasma parameters are $n_{e,0} = 3.9 \times 10^{19}$ m^{-3}, $T_{e,0} = 900$ eV, $I_{\rm pl} = 101$ kA, $B_{\rm tor} = 2.05$ T, $Z_{\rm eff} = 2.6$, $v_{\rm pellet} = 986$ m/s, $m_{\rm pellet} = 2.0 \times 10^{19}$ atoms, $r_{\rm pellet} = 0.4$ mm.

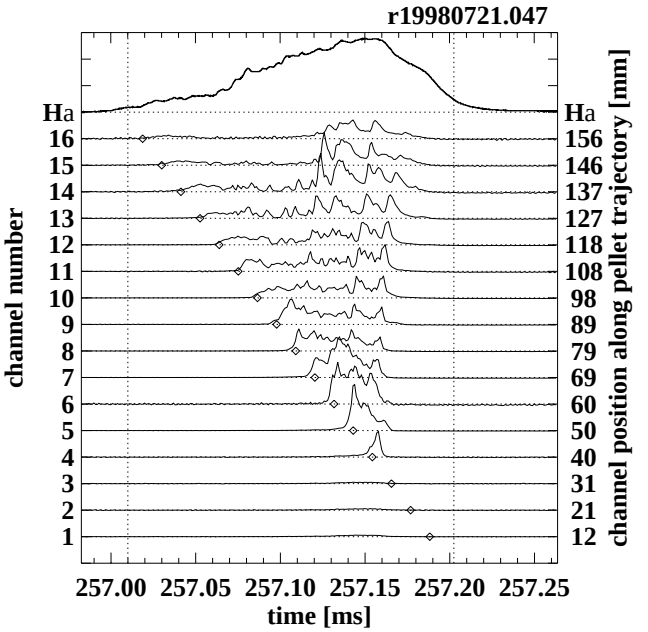

FIG. 4. Example of the pellet ablation process as observed by the new fiber-array diagnostic plotted in the same way as in Fig. 2. In this case the pellet was injected in a centrally ECH heated plasma. Clearly the secondary peaks have much higher amplitude on the outer channels than the primary pulse (channels 10–16). The pellet and plasma parameters are $n_{e,0} = 5.2 \times 10^{19}$ m^{-3}, $T_{e,0} = 1450$ eV, $I_{\rm pl} = -81.5$ kA, $B_{\rm tor} = 2.01$ T, $Z_{\rm eff} = 2.0$, $v_{\rm pellet} = 852$ m/s, $m_{\rm pellet} = 2.0 \times 10^{19}$ atoms, $r_{\rm pellet} = 0.4$ mm, ECH power = 320 kW.

using the wide angle H_α signal is 17 ± 1 cm while the new diagnostic gives a penetration of $\approx 13.0 \pm 0.5$ cm.

Up to now the secondary peaks do not seem to reproduce in detail. They do not develop at regular time intervals or positions, and have different magnitudes and lifetimes, even with very similar plasma and pellet conditions.

We have observed the neutral cloud surrounding the pellet using a new diagnostic. For pellet injection in a cold plasma ($T_e \leq 400$ eV) the observed cloud size was on average 12 ± 5 mm (see Fig. 2).

In hotter plasmas the cloud size increases and parts of it start drifting away.

In most models the radial cloud size is assumed to be determined by the ionization radius r_i. Using an expression derived by Parks [7] we obtain $r_i \approx 1$ to 3 mm for RTP. This is significantly smaller than the observed ablation cloud.

The observation of the secondary peaks is interpreted as a not fully ionized cloud moving away from the pellet through the plasma.

The movement has a velocity component along the pellet trajectory but in opposite direction as the pellet velocity. A major radial velocity of 3.5 to 10 km/s can be deduced from the signals.

The results obtained with this diagnostic may be helpful in determining the importance of movements of the ablation cloud. The possibility of these effects have been pointed out by Kaufmann *et al.* [8] and Rozhansky *et al.* [9].

In the literature two types of drifts have been considered in the ablation cloud. Because of the Lorentz transformation the pure B field in the laboratory frame is converted to an electric field $\mathbf{E} = \mathbf{v}_{\rm pellet} \times \mathbf{B}_{\rm tor}$ in the pellet frame. This can give two effects [3]. Under open circuit conditions (case 1) it causes a polarization in the cloud giving rise to an $E \times B$ drift with magnitude $\mathbf{v}_{\rm drift} = \frac{\mathbf{E}\times\mathbf{B}}{\mathbf{B}^2} = \frac{\mathbf{v}_{\rm pellet}\times\mathbf{B}\times\mathbf{B}}{\mathbf{B}^2} = \mathbf{v}_{\rm pellet}$ in the lab frame. This drift is in the direction of the pellet velocity and causes the ablation cloud to stick to the pellet. This is not consistent with the observations.

In short circuit conditions (case 2) no large charge separation can build up but a continuous current is running through the ablation cloud. This current density j can be described by the local E field and the local conductivity σ as $\mathbf{j} = \sigma\mathbf{E}$. If no external forces on the particles (with charge q) are present, the only ones are the electric and magnetic field, so the force equation reads $f = 0 = q\mathbf{E} + q\mathbf{v}_{\rm cloud} \times \mathbf{B}$ so $\mathbf{j} \times \mathbf{B} = -\sigma\mathbf{v}_{\rm cloud}\mathbf{B}^2$. This force causes a movement of the ablation cloud away from the pellet, and, in fact, lets the cloud stick to the magnetic

field, stopping its movement in radial direction. Since we observe the cloud to move backward towards the plasma edge also, this picture cannot be true.

Rozhansky considered a third possibility, the grad **B** drift [9]. Because of the gradient in the toroidal field a drift velocity of $\mathbf{v}_{\nabla\mathbf{B}} = \frac{1}{2} v_\perp r_L \frac{\mathbf{B}\times\nabla\mathbf{B}}{\mathbf{B}^2}$ occurs (here $v_\perp$ is the velocity of the particles perpendicular to the field lines, and r_L is the Larmor radius). Because of the high collisionality particles cannot complete an orbit around the torus, so the drift is not compensated by the rotational transform. This causes a polarization in opposite direction, compared to case 1, that starts to increase linearly with time as $\mathbf{E} = \mathbf{v}_{\nabla\mathbf{B}} n_e q t$. This causes an $\mathbf{E} \times \mathbf{B}$ drift in a direction opposite to the pellet velocity, with linearly increasing velocity. After inserting RTP values in the formulas given by Rozhansky (Ref. [9], Eq. 24) a velocity of $\approx 5-10$ km/s is expected. This is in good agreement with the observations.

Another still unexplained feature of pellet injection is the striations, a modulation of the observed H_α signals. Two basic ideas have been developed to explain this phenomenon. One was proposed by Neuhauser [10] and assumes that the pellet periodically leaves the shielding cloud. For RTP this would give a typical cloud radius of 1.5–2.5 mm, calculated from striations in the observed H_α signals. This is not in agreement with the cloud size which has been measured.

However, an alternative explanation is possible when the drift of the ablation cloud is taken in consideration. Then the ablation cloud may be periodically drifting away from the pellet (at a velocity up to 1 order of magnitude higher than the pellet velocity), leaving it unprotected and exposed to the hot plasma and causing a modulation in the ablation rate independent of the ratio cloud size/v_{pellet}.

An altogether different mechanism was proposed by Andelfinger [11] and further investigated by Pégourié and Dubois [12], which assumes that less energy is available at rational q surfaces to ablate the pellet. The observations shown in this Letter do not support this hypothesis.

A consequence of the presented results is that it is not to be expected that the H_α signal is proportional to the local fueling rate. Also it follows that it is difficult to determine pellet penetration using the wide angle H_α signal. This gives only a maximum possible penetration by assuming that no matter drifts away from the pellet. Better estimates for low field side injection are obtained by using a (photographic) camera.

If the ablation cloud exists for some time after the complete ablation of the pellet also, determination of the lifetime of the pellet is impossible with the wide angle H_α diagnostic (see Fig. 4).

In conclusion, a new diagnostic has been build to observe pellet ablation in the RTP tokamak. This diagnostic has proven to be well suited to observe movements of (parts of) the pellet ablation cloud. In the absence of such a drift it can be used to determine the ablation cloud size and velocity during the ablation process. We have observed a drifting of the ablation cloud away from the pellet with a velocity component in major radius direction of 3.5 to 10 km/s. The direction and velocity of this cloud can be explained using the mechanism proposed by Rozhansky [9]. This phenomenon has never been observed directly before [3].

The observations emphasize the importance of inboard side pellet injection (for which the observed drift would improve the possibility of fueling the plasma center).

This work was done under the Euratom-FOM association agreement, with financial support from NWO and Euratom.

[1] L. R. Baylor *et al.,* Nucl. Fusion **32**, 2177 (1992).
[2] A. J. H. Donné and the RTP-Team, Plasma Phys. Rep. **20**, 192 (1994).
[3] S. L. Milora, W. A. Houlberg, L. L. Lengyel, and V. Mertens, Nucl. Fusion **35**, 657 (1995).
[4] M. N. A. Beurskens *et al.,* Rev. Sci. Instrum. **68**, 721 (1997).
[5] J. H. Rommers, A. J. H. Donné, F. A. Karelse, and J. Howard, Rev. Sci. Instrum. **68**, 1217 (1997).
[6] G. M. D. Hogeweij *et al.,* Phys. Rev. Lett. **76**, 632 (1996).
[7] P. B. Parks, Nucl. Fusion, **20**, 311 (1980).
[8] M. Kaufmann, K. Lackner, L. Lengyel, and W. Schneider, Nucl. Fusion **26**, 171 (1986).
[9] V. Rozhansky, I. Veselova, and S. Voskoboynikov, Plasma Phys. Controlled Fusion **37**, 399 (1995).
[10] J. Neuhauser and R. Wunderlich, Max-Planck-Institut für Plasmaphysik, Garching bei München, Report No. IPP 5/30, 1989.
[11] C. Andelfinger *et al.,* Max-Planck-Institut für Plasmaphysik, Garching bei München, Report No. IPP 1/219, 1983.
[12] B. Pégourié and M. A. Dubois, Nucl. Fusion **29**, 745 (1989).